
Intrinsic Non-stationary Covariance Function for Climate Modeling

Chintan A. Dalal

Department of Computer Science
Rutgers, The State University of New Jersey
chintan.dalal@rutgers.edu

Vladimir Pavlovic

Department of Computer Science
Rutgers, The State University of New Jersey
vladimir@cs.rutgers.edu

Robert E. Kopp

Department of Earth & Planetary Sciences
Rutgers, The State University of New Jersey
robert.kopp@rutgers.edu

Abstract

Designing a covariance function that represents the underlying correlation is a crucial step in modeling complex natural systems, such as climate models. Geospatial datasets at a global scale usually suffer from non-stationarity and non-uniformly smooth spatial boundaries. A Gaussian process regression using a non-stationary covariance function has shown promise for this task, as this covariance function adapts to the variable correlation structure of the underlying distribution. In this paper, we generalize the non-stationary covariance function to address the aforementioned global scale geospatial issues. We define this generalized covariance function as an intrinsic non-stationary covariance function, because it uses intrinsic statistics of the symmetric positive definite matrices to represent the characteristic length scale and, thereby, models the local stochastic process. Experiments on a synthetic and real dataset of relative sea level changes across the world demonstrate improvements in the error metrics for the regression estimates using our newly proposed approach.

1 Introduction

Covariance functions are a key element in the regression of geospatial data (kriging). Designing a covariance function that can capture the geospatial random field of natural processes is useful for understanding the changes occurring in climate related variables. For example, ongoing sea level changes provide an important context for understanding future coastal flood risks [1]. However, most of the climate related datasets at a global scale suffer from statistical issues of non-stationarity and non-uniformly smooth spatial boundaries. In this paper, we design a covariance function which addresses these issues in the datasets.

Stochastic processes of complex systems at a global scale are known to have a regional geophysical variability. For example, the local sea-level changes occurring near Northern Europe are primarily dominated by the physics of the Glacial-isostatic adjustment, while the local sea-level changes occurring near Japan are dominated by the tectonics [2]. Such regional variations can be modeled using the non-stationary covariance function (Figures 1(a,b) depicts these issues).

One of the important modeling issues in the complex geospatial dataset at a global scale is knowing the boundaries of the regional geophysical variability. Addressing this issue, which we call the non-uniformly smooth spatial boundary issue, aids in modeling the non-stationary covariance function by capturing the underlying correlation structure of a region. This paper addresses this issue for kriging.

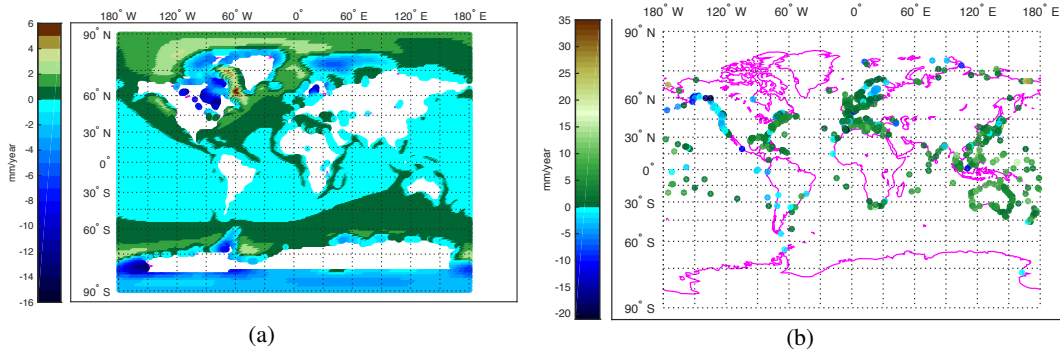


Figure 1: Experimental datasets. (a) Synthetic data of the relative sea-level change from the Glacial-isostatic adjustment model, and (b) real tide gauge data of the rate of change of the sea level during the last 20 years across the world.

For standard kriging models (GP), the methods given in [3] are widely used in many climate models, including models of the sea level data, because it gives a non-parametric method for analyzing such a geospatial random field. Such a model can be completely defined by its covariance function, and it learns the hyper-parameters of the designed covariance function directly from the training data without making any parametric assumptions about the data.

To model the non-stationarity of the stochastic process, [4, 5, 6, 7] devised a non-stationary covariance function. These methods use spatially evolving smooth kernels to represent the characteristic length scale (CLS) of the covariance function, which, in turn, models the local correlation structure of the global scale stochastic process. From these methods, [4] is the most promising approach for climate data, as its model is entirely in the non-parametric GP framework. Even so, it uses a homogeneous set of hyper-parameters to ensure the smoothness of the CLS in the input space. We show in our experiments that using a homogeneous set of hyperparameters is inefficient for the global-scale complex systems.

Non-stationarity has also been addressed by [8]. They use a multi-resolution basis function, fixed rectangular grid, and explicit thresholding scheme. The approach of setting fixed grids renders this method unviable for datasets with non-uniformly smooth boundaries. While [4] validates their model on precipitation estimates in Colorado (USA), [8] uses the daily ozone rate in the Midwest. Both of these datasets are locally dense, and, in turn, do not address the global scale climate data issues.

In the literature of estimating global scale sea-level changes, techniques given by [9] use a Kalman filter model, and [2] use a mixture of GPs at various regional resolutions. However, these methods fail to tightly couple the local and global estimates in the spatial dimension. Additionally, these methods rely on the domain knowledge and a parametric framework.

In this paper, we propose a covariance function to model the data and address the aforementioned issues at a global scale, and we call this covariance function the intrinsic non-stationary covariance function. We use intrinsic statistics [10] on the space of the CLS to capture the non-uniformly smooth spatial boundaries for the non-stationarity. Furthermore, we provide an algorithm for kriging using the proposed intrinsic covariance function, and we validate its applicability on two global scale datasets.

2 Covariance functions used in climate modeling

In this section, we provide relevant background about stationary and non-stationary covariance functions used in kriging, which helped in the development of our proposed framework of the intrinsic non-stationary covariance function. The standard kriging (GP) model tries to recover the underlying function, f , where $y_i \sim f(x_i) + \eta$, from n observed data points $\{(x, y)\}_{i=1}^n$. The learned model is then used to compute the predictive distribution $p(y^*|x^*, f)$ for a test point x^* . Here, $x \in \mathbb{R}^d$ are points in the input space of dimension d , $y \in \mathbb{R}$ are observed values, and η is observed noise. In our problem setting, x represents the 2D spatial coordinates (latitude and longitude) and y represents the rate of change of the sea level at x .

Assuming Gaussian noise $\eta \sim \mathcal{N}(0, \sigma_n^2)$ with a constant variance term σ_n^2 , the predictive distribution is then given by $\mathcal{N}(\mu, \sigma^2)$, where: $\mu = k_*^T (K + \sigma_n^2 I)^{-1} y$, $\sigma^2 = k_{**} - k_*^T (K + \sigma_n^2 I)^{-1} k_* + \sigma_n^2$, $K(i, j) = k(x_i, x_j)$, $k_*(i) = k(x_*, x_i)$, $k_{**} = k(x_*, x_*)$, $y = (y_1, \dots, y_n)^T$, and I is the identity matrix [3]. Here, $k(x_i, x_j)$ is the covariance function which we are interested in modeling.

2.1 Stationary covariance function

For kriging, the correlation structure of the data is commonly modeled as a stationary covariance function when the underlying stochastic process of a function (f) is assumed to be stationary. A stationary isotropic covariance function that is motion and translation invariant can be defined as $k(x_i, x_j) = \phi(\frac{d^2(x_i, x_j)}{l^2})$. Here, $\phi : [0, \infty) \rightarrow \mathbb{R}$ is a positive definite function, l^2 is the CLS, and $d(x_i, x_j)$ is the distance function (in geophysical measurements, this is commonly angular distance). As can be seen from the construction, when the CLS is large the correlation between the input space points is spatially small, and vice versa. In other words, the points that are far apart have a small effect on the inference step.

When the CLS is differing with respect to the input space dimensions, d , the covariance function is called an anisotropic covariance function. One such form of this covariance function is given by $k(x_i, x_j) = \phi(d(x_i, x_j)^T (\Sigma)^{-1} d(x_i, x_j))$. Here, the CLS, $\Sigma : \mathbb{R}^d \rightarrow S^+(d, \mathbb{R})$, can be decomposed into $\Sigma = \Gamma^T D \Gamma$. Γ is a $d \times k$ column vector and it gives the direction of relevance, D is a $k \times k$ diagonal matrix and it gives the magnitude of relevance, and k is the relevant number of axis-aligned dimensions.

To date, various ϕ for $k(\cdot, \cdot)$ have been proposed. For spatial statistics, the Matérn covariance function is a standard choice due to its flexibility in capturing the varying smoothness of the underlying distribution:

$$k(x_i, x_j) = K_S(\nu, \sqrt{Q_{ij}}) = \frac{(\sqrt{2\nu Q})^\nu K_\nu(\sqrt{2\nu Q})}{\sigma_f^{-2} 2^{\nu-1} \Gamma(\nu)}, \quad (1)$$

where $Q_{ij} = \frac{d^2(x_i, x_j)}{l^2}$, ν is the smoothness hyperparameter that controls the differentiability of the function, σ_f is the signal variance, K_ν is the modified Bessel function, and $\Gamma(\nu)$ is the gamma distribution.

2.2 Non-stationary covariance function

The non-stationary covariance function can be modeled using a covariance function that varies its CLS with respect to the input point of interest. The non-parametric model form for such a covariance function is given by $k(x_i, x_j) = \phi(Q_{ij})$, $Q_{ij} = d(x_i, x_j)^T (\frac{\Sigma_i + \Sigma_j}{2})^{-1} d(x_i, x_j)$, and $\Sigma_i := \Sigma(x_i) = \Gamma(x_i)^T D(x_i) \Gamma(x_i)$. For this non-stationary covariance function to be valid, [6] shows (using a convolution of kernels) that $\Sigma(x) : \mathbb{R}^d \rightarrow S^+(d, \mathbb{R})$ should be spatially evolving smooth kernels of symmetric positive definite matrices.

A closed-form solution of the nonstationary Matérn covariance function is given by [4] as:

$$k(x_i, x_j) = K_{NS}(x_i, x_j) = \frac{2^{d/2} \sigma_f^2 |\Sigma_i|^{1/4} |\Sigma_j|^{1/4}}{|\frac{\Sigma_i + \Sigma_j}{2}|^{1/2}} K_S(\nu, \sqrt{Q_{ij}}). \quad (2)$$

Intuitively, Equation (2) indicates that the covariance between two observed values (y_i) is affected by the convolution (arithmetic average) of the local covariates (kernels) at the input locations (x_i). Consequently, this results in a variable CLS at the target values (y^*).

2.3 Spatially evolving kernels for the characteristic length scales

For modeling the CLS, [6] uses a predetermined area of the ellipse, [11] uses B-splines, and [4] uses a stationary GP. All of these methods capture the underlying local correlation of the data using N neighbors of x_i . In this paper, we are interested in models that ensure a locally smooth manifold

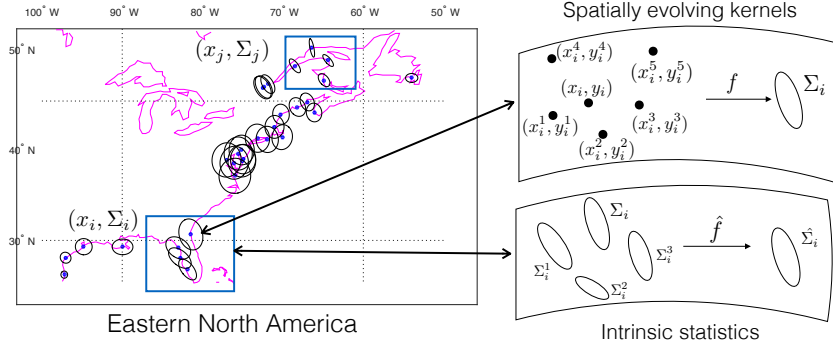


Figure 2: Proposed framework for the intrinsic non-stationary covariance function.

of Σ_i , which lies in the space of positive definite matrices $S^+(d, \mathbb{R})$ in a non-parametric fashion, while still being entirely in a GP framework. [4] proposes the following eigen-decomposition of Σ_i for the spatial data:

$$\Gamma(x_i) = \begin{bmatrix} \frac{u}{l_{uv}} & \frac{-v}{l_{uv}} \\ \frac{v}{l_{uv}} & \frac{u}{l_{uv}} \end{bmatrix}, D(x_i) = \begin{bmatrix} \log(\lambda_1) & 0 \\ 0 & \log(\lambda_2) \end{bmatrix}, l_{uv} = \sqrt{u^2 + v^2}. \quad (3)$$

The eigen decomposition parameters $\{u, \lambda_1\}_i$ are each, in turn, modeled using an independent stationary GP in the latitude dimension of x_i , and $\{v, \lambda_2\}_i$ using an independent stationary GP in the longitude dimension of x_i . All four independent GPs have their own sets of hyperparameters.

3 Intrinsic non-stationary covariance function

In this section, we first propose our model of the covariance function (intrinsic non-stationary covariance function), then give background for the intrinsic statistics that we employ to construct the intrinsic non-stationary covariance, and finally provide an algorithm for its implementation in kriging.

In order to improve the model of the non-stationary covariance function that captures the variable regional information, while still maintaining a non-parametric model, we propose a new class of covariance functions and define this class as an intrinsic non-stationary covariance function.

Definition 1. An intrinsic non-stationary covariance function $k(\cdot, \cdot)$ assumes the form $k(x_i, x_j) = \phi(Q_{ij})$, where $Q_{ij} = d(x_i, x_j)^T (\psi_{ij})^{-1} d(x_i, x_j)$ and $\psi_{ij} := \psi(\Sigma_i, \Sigma_j)$.

Here, $\psi : S^+(d, \mathbb{R}) \rightarrow S^+(d, \mathbb{R})$ is an objective function of the form:

$$\psi(\Sigma_i, \Sigma_j) := \operatorname{argmin}_{\bar{\Sigma}} \sum_{\{i,j\} \in \mathcal{N}} d^2(\bar{\Sigma}, \Sigma_{\{i,j\}}), \quad (4)$$

where $\bar{\Sigma}$ is the CLS for the intrinsic non-stationary covariance function, $d^2(\cdot, \cdot)$ is the intrinsic distance metric, \mathcal{N} is the neighbors (including itself) of the geospatial point of interest i, j , and $d(x_i, x_j)$ is the distance in the input space.

In our study, the aim of the objective function $\psi(\cdot, \cdot)$ is to model the regional geophysical CLS of the underlying stochastic process. Intuitively, $\bar{\Sigma}$ represents the intrinsic mean of the CLS at the input points $\{x_i, x_j\}$, and it incorporates the regional CLS in its convolution step for the intrinsic covariance function.

There are two important factors in modeling this function ψ :

1. Finding the neighborhood points that represent the regional information.
2. Finding a representative of the CLS that describes the statistics (up to second-order) for the region of interest.

Figure 2 depicts these two factors, and Section 3.2 gives one such method to construct these classes of functions.

Theorem 1. *The intrinsic non-stationary covariance function, as defined above, is a valid non-stationary covariance function.*

Proof. [6] shows that the construction of a covariance function using a moving average specification (i.e., convolution of kernels) leads to a non-stationary process. In our construction (Equation 4) we specify the convolution of kernels on a smooth manifold, preserving the properties of symmetric positive definite matrices, and, in turn, obtaining a non-stationary process definition of [6] with a positive definiteness of the covariance function. \square

3.1 Intrinsic Statistics for the characteristic length scales

To compute the objective function ψ for the space of spatially smooth kernels $(\{\Sigma_i\}_{i=1}^N)$, we assume that ψ lies on the Riemannian manifold \mathcal{M} of positive definite matrices $S^+(d, \mathbb{R})$. The Riemannian manifold is assumed to be geodesically complete and endowed with a canonical affine connection. [12] and [13] derived explicit forms of the geodesic distance on this manifold as: $d(\Sigma_i, \Sigma_j) = \sqrt{\frac{1}{2} \sum_{i=1}^d \log^2(\eta_i)}$, where η_i denotes the d eigenvalues of the matrix $(\Sigma_i^{-1/2} \Sigma_j \Sigma_i^{-1/2}) \in S^+$.

[14] defined the empirical Riemannian mean $\bar{\Sigma} \in S^+(d, \mathbb{R})$, and [15] gave an iterative form of $\bar{\Sigma}$ as a local minimum of the objective function $\lambda^2 : S^+(d, \mathbb{R}) \rightarrow \mathbb{R}^+$:

$$\lambda^2(\Sigma_1, \dots, \Sigma_N) = \frac{1}{N} \sum_{k=1}^N d^2(\Sigma_k, \bar{\Sigma}). \quad (5)$$

Each of the N normal distributions $p(\cdot | \Sigma_k)$ is associated with a unique tangent vector $\beta_k \in S(d, \mathbb{R})$, such that $\bar{\Sigma}$ is mapped onto Σ_k by an exponential map $\exp_{\bar{\Sigma}}(\beta_k) = \bar{\Sigma}^{1/2} \exp(\bar{\Sigma}^{-1/2} \beta_k \bar{\Sigma}^{-1/2}) \bar{\Sigma}^{1/2}$. The covariance matrix of a set of covariance matrices itself (i.e., in our model this is a covariance of a set of the CLS) is then defined as:

$$\Lambda_{\bar{\Sigma}} = \frac{1}{N-1} \sum_{k=1}^N \beta_k \beta_k^T. \quad (6)$$

The covariance of the set of the CLS gives us a measure by which to evaluate the properties of its distribution on a manifold. For example, when the $tr(\Lambda)$ is small, it means that the set of covariances (CLS) are from the same normal distribution $\mathcal{N}(\Sigma | \bar{\Sigma}, \Lambda)$ and are highly correlated.

Note the similarity in the variable N of (5) and $\{\{i, j\} \in \mathcal{N}\}$ of (4), which shows that ψ_{ij} is in fact the intrinsic Riemannian mean $\bar{\Sigma}$.

3.2 Algorithm for the intrinsic non-stationary covariance function

Algorithm 1 Kriging for the Intrinsic Non-stationary Covariance Function

- 1: **Input:** Training set $\{(x, y)\}_{i=1}^n$, Test points $\{x^*\}_{i=1}^m$.
 - 2: **Output:** Predictive densities $p(y^* | x^*)$.
 - 3: Initialize estimates of Σ_i using Equation (3).
 - 4: Find the characteristic length scale ψ_{ij} using Algorithm 2.
 - 5: Compute the intrinsic nonstationary covariance function using Equation (2).
 - 6: Compute the GP using $p(y^* | x^*, f) \sim \mathcal{N}(\mu, \sigma)$.
-

Algorithm 1 describes our framework for implementing the intrinsic non-stationary covariance function, and Figure 2 depicts this general framework. We first obtain initial smooth estimates of the CLS (Σ_i) by Equation (3), and then we update Σ_i with the aim of modeling the intrinsic function ψ_{ij} using our approach proposed in Algorithm 2. Our method maintains the appropriate smoothness in the latent space of Σ_i due to the second-order intrinsic statistics on the Riemannian manifold. Additionally, our method captures the correlation of the Σ_i in its intrinsic latent space that the initial estimate failed to capture. Hence, the estimates for the CLS around sharp discontinuities

Algorithm 2 Intrinsic Characteristic Length Scale

- 1: **Input:** $\{x_i, x_j\}, \{x_k, \Sigma_k\}_{k=1}^n$.
 - 2: **Output:** ψ_{ij} .
 - 3: Find K nearest neighbors \mathcal{N}_i for x_i and \mathcal{N}_j for x_j in the input space.
 - 4: Remove the Σ_i 's from $\{\Sigma_i\}_{i \in \mathcal{N}_i}$, such that, $|tr(\Lambda_i)| < \text{threshold}$.
 - 5: Find $\bar{\Sigma}_i$ using $\lambda^2(\{\Sigma_i\}_{i \in \mathcal{N}_i})$ for Eq. 5.
 - 6: Remove the Σ_j 's from $\{\Sigma_j\}_{j \in \mathcal{N}_j}$, such that, $|tr(\Lambda_j)| < \text{threshold}$.
 - 7: Find $\bar{\Sigma}_j$ using $\lambda^2(\{\Sigma_j\}_{j \in \mathcal{N}_j})$ for Eq. 5.
 - 8: Find ψ_{ij} using $\lambda^2(\bar{\Sigma}_i, \bar{\Sigma}_j)$
-

and separated regions of the spatial data field are improved, as shown in Figure 3. Finally, the CLS (ψ_{ij}) is used in Equation (2) for the GP regression model.

For step (3) of Algorithm 1, [4] bound the $\{\Sigma_i\}_{i=1}^N$'s to achieve the required smoothness and used the arithmetic mean to convolve Σ_i and Σ_j for its covariance function. We used the empirical Riemannian mean rather than the arithmetic mean and, therefore, are free from fixing the bounds on the initial estimates of $\{\Sigma_i\}_{i=1}^N$. This allows the variable smoothness in Equation (2) to naturally evolve in the space of symmetric positive definite matrices. Note, the thresholds of variance are bounded in the space of $\{\Sigma_i\}_{i=1}^N$ and are not directly dependent on the input space. Additionally, [16] shows that the arithmetic mean causes larger determinants (than the original determinant) in the space of $S^+(d, \mathbb{R})$, which the Riemannian mean avoids.

Algorithm 2 uses two levels of nearness measures: 1) the usual distance metric directly on the input space that measures spatial proximity, and 2) the intrinsic statistics of Σ_i that measure its proximity on the manifold. Here, we used $|tr(\Lambda_i)|$ to measure the correlation of the neighboring Σ_i 's for its simplicity, but one could also use the K -nearest neighbors in the space of Σ_i s. It would be worth exploring how the different statistical measures on the manifold of the CLS space could improve the kriging estimates when sharp jumps exist in the underlying distribution.

For example, a CLS computation of a geospatial location that is close to the boundary of its geophysical region is less reliable when it is the function of its input space alone (i.e., Σ_i in Algorithm 1, Step 3). However, when the additional information of the neighboring CLS is incorporated into the model (i.e., Algorithm 2, Step 4 and 5), one could potentially recover the CLS of the boundary points that is closer (Equation 5) to the CLS representative of its associated region. We show in the experimental section that this approach of Algorithm 2 is particularly useful for analyzing climate models.

For the initialization of the CLS in Algorithm 1, Step (3), one can use the numerical implementation of either [4], [6], or [11]. In our experiments, we used [4], because the empirical testing showed that it gave the best results for our application. Similarly, we used the numerical implementation of [13] for the intrinsic statistics (Equations (5) and (6)).

The K for the nearest neighbors and the threshold for the variance in Alg. 2 are found using the 5-fold Cross Validation. To find the GP hyperparameters, for step (1) and step (5) in Alg. 1, we use a Markov Chain Monte Carlo (MCMC) sampling scheme that is similar to the one outlined in [5].

4 Experiments on climate related data

To gain insight into the applicability of our proposed covariance function, we implemented and compared kriging with three different covariance functions: the widely used stationary anisotropic Matérn covariance function (statGP) of [17], the baseline non-stationary covariance function (NSGP) of [4], and the intrinsic non-stationary covariance function (iNSGP) that we propose in this paper. These methods were evaluated using two standard performance measures (as described below) for kriging. The three datasets used are: the smooth $2d$ simulated dataset (SIM) given in [4], the geophysics driven synthetic¹ data (GIA) as modeled in [18], and the global-scale complex naturally occurring real² dataset (TG) collected in [19].

¹http://www.psmsl.org/train_and_info/geo_signals/gia/peltier/

²<http://www.psmsl.org/data/obtaining/>

Table 1: Evaluations of the simulated (SIM), synthetic (GIA), and real (TG) datasets. GIA and TG dataset results are in the units of mm/year.

Methods	SIM		GIA (All)		GIA (Reg.1)		TG (All)	
	sMSE	nLPD	sMSE	nLPD	sMSE	nLPD	sMSE	nLPD
StatGP	0.0240	0.311	0.58	3.08	1.57	19.23	0.85	2.81
NSGP	0.0237	0.278	0.56	2.00	1.24	7.30	0.75	2.82
iNSGP	0.0235	0.271	0.54	1.94	1.03	6.90	0.71	2.78

The Simulated Dataset. For this study, we are interested in comparing our method with the $2d$ simulated functions that have been previously used in the non-stationary covariance function literature. The experimental set up is given in [4]. Even though the simulation function is non-stationary, it is fairly smooth and homogeneous, and it lacks the complex regional geophysics that is usually encountered in global-scale climate related data.

The Synthetic Dataset. For this study, we are interested in modeling the global-scale geophysical signal that is present in the climate datasets (such as tide gauge data). This synthetic dataset enables us to compare the three covariance functions (statGP, NSGP, iNSGP) with known geophysics boundaries.

One such widely modeled geophysical signal is the Glacial-isostatic adjustment (GIA) model. We used the signal modeled in GIA [18], which gives the difference in the height between the sea surface and solid earth. Figure 1(a) shows the distribution of the underlying distribution (y) after masking out the land mass. To examine the robustness of our proposed model, the experimental setup includes 25 independent runs of the GIA data. For each run, we randomly sampled 315 training points, added Gaussian noise ($\eta = 0.2$) to sea level measurements, and tested on 946 independent random sampled points.

The Real Dataset. For this study, we are interested in a global-scale climate variable that contributes to future climate related risks, is known to have non-stationarity, and has complex regional geophysics in its dataset. Hence, we used tide gauge sites measuring relative sea level measurements across the coastal areas of the globe (see Figure 1(b)). From the dataset given in [19], 747 locations were selected because they had consistent temporal records from the years 1993 to 2012. To focus our study on the geo-spatial set up, we used 747 locations of tide gauge sites to construct the rate of change of the sea level (mm/year), where the annual sea level rate of change was obtained from linear regression estimates in the temporal dimension. The experimental set up then includes 25 independent runs with randomly sampled 374 and 373 locations for respectively the training and test set.

Evaluation metrics. We report performance with respect to two widely adopted metrics in kriging: the standardized mean squared error (sMSE) and the negative log predictive density (nLPD). sMSE measures the point estimate errors in the predictions and is given by: $sMSE = n^{-1} \sum_{i=1}^n \text{var}(y)^{-1} (y_i - y_i^*)^2$, where n is the number of test points, y_i^* is the predictive mean at input space x_i , and $\text{var}(y)$ is the sample variance. nLPD measures not just the point estimates error, but also the error variance of the predictions and is given by: $nLPD = -n^{-1} \sum_{i=1}^n \log(p(y_i|x_i))$.

5 Results

Table 1 summarizes the performance for the three covariance functions (statGP, NSGP, and iNSGP) when implemented on the three datasets (SIM, GIA, and TG). The performance of iNSGP is particularly improved for the GIA and TG datasets, while it does not show much of an improvement over NSGP for the SIM dataset. This is mainly because the SIM dataset is fairly smooth. Furthermore, the SIM data does not suffer from the issue of a non-uniformly smooth spatial boundary (regional geophysics) that is present in GIA and TG datasets Fig 1(a).

For example, Fig 3(a) shows the true values of GIA data near the Barent sea (Reg.1), which is a marginal sea of the Arctic ocean. The CLS estimates for this region (which is parametrically plotted as ellipses) from statGP, NSGP, and iNSGP are shown in Fig 3(b,c,d). Note the differences in the shape of the ellipses numbered (1,2,3) in Fig 3(b,c,d). These points (1,2,3) correspond to the geospatial boundary points of the regions (1,2,3) in Fig 3(a). While statGP has the same shape for all of the points, NSGP shows some variation in its shape. Even so, they are largely similar. On the other hand, iNSGP has a distinct variation in the the points (1,2,3) and well represents the

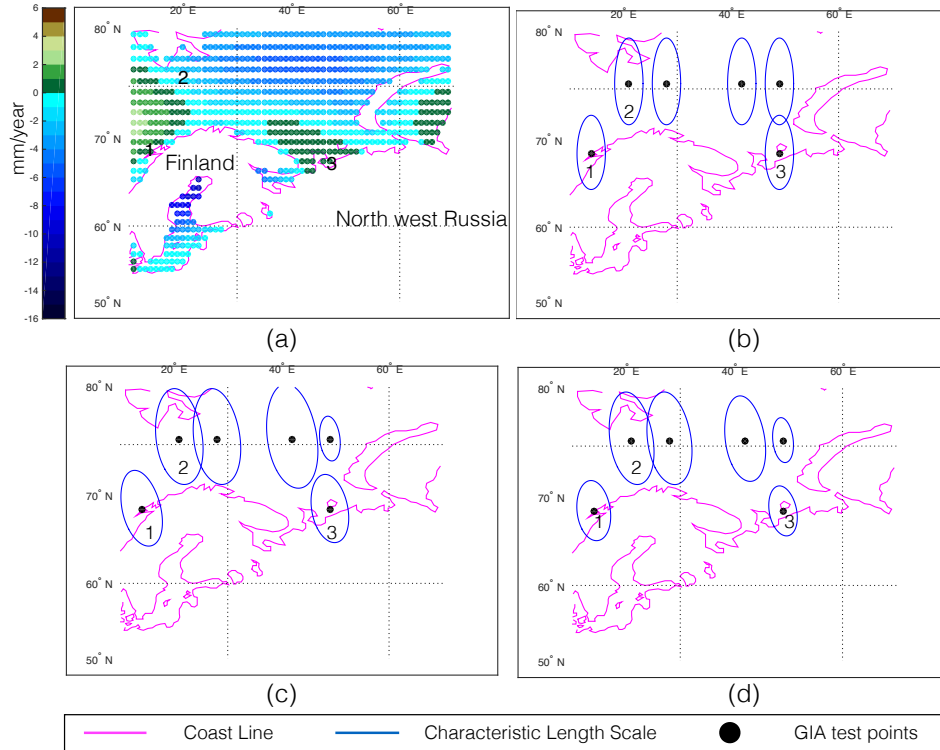


Figure 3: GIA dataset around Barrent sea (Reg.1) (a) GIA data (true values), (b) Stationary GP (statGP) characteristic length scale (CLS), (c) Non-stationary GP (NSGP) CLS, and (d) Intrinsic non-stationary GP (iNSGP) CLS.

differences in these three regions. This is explained by the superior performance (Tab. 1) of iNSGP over NSGP and statGP (particularly in the GIA Reg.1).

Table 1, shows the average values for the error metrics. The maximum standard deviation in sMSE for SIM was 0.003, for GIA was 0.02, and for TG was 0.5. For each of these runs, iNSGP performed as well as NSGP for the SIM dataset, and outperformed NSGP and statGP for the TG and GIA datasets. The error values for the SIM dataset when applying the methods of StatGP and NSGP were similar to the error values found in [4].

From all three datasets, the real dataset (TG) shows the most improvement in its error metric when applying the iNSGP method. The high improvement is because TG has large variability in the regional geophysics; therefore, the intrinsic non-stationary covariance function is able to better model the underlying true distribution than the stationary and non-stationary covariance functions.

6 Discussion and Concluding Remarks

We introduced a new class of covariance functions, which we call an intrinsic non-stationary covariance function. This covariance function is especially useful in modeling global scale geospatial datasets that have a non-stationary process and non-uniformly smooth spatial boundaries due to regional geophysics. We developed a framework to apply this covariance function for kriging. Using the sea level dataset from the Glacial-isostatic adjustment model and tide gauge measurements, we demonstrated our framework's improved performance in kriging when compared with the non-stationary covariance function.

There are many facets of implementation of the intrinsic non-stationary covariance function that could be undertaken in the future. One of the important issues, especially outside of the geo-spatial community, is large datasets. Specifically, one can use sparse regression techniques [20] and a computationally cost effective metric for the intrinsic statistics on the positive definite matrices of the characteristic length scale [16] to deal with large datasets.

Other climate related variables, such as temperature and precipitation records, face similar modeling issues as the sea level dataset that we used for our application. Future work will explore the application and methods of our intrinsic covariance function to such geospatial datasets, with the larger goal of aiding in the assessment of future climate related risks.

References

- [1] John A Church, Peter U Clark, Anny Cazenave, Jonathan M Gregory, S Jevrejeva, A Levermann, MA Merrifield, GA Milne, RS Nerem, PD Nunn, et al. Sea level change. *Climate change*, pages 1137–1216, 2013.
- [2] Robert E Kopp. Does the mid-atlantic united states sea level acceleration hot spot reflect ocean dynamic variability? *Geophysical Research Letters*, 40(15):3981–3985, 2013.
- [3] Carl Edward Rasmussen and CKI Williams. Gaussian processes for machine learning. 2006. *The MIT Press, Cambridge, MA, USA*, 38:715–719, 2006.
- [4] C Paciorek and M Schervish. Nonstationary covariance functions for gaussian process regression. *Advances in neural information processing systems*, 16:273–280, 2004.
- [5] Christian Plagemann, Kristian Kersting, and Wolfram Burgard. Nonstationary gaussian process regression using point estimates of local smoothness. In *Machine learning and knowledge discovery in databases*, pages 204–219. Springer, 2008.
- [6] Dave Higdon, J Swall, and J Kern. Non-stationary spatial modeling. *Bayesian statistics*, 6(1):761–768, 1999.
- [7] M. Stein. *Interpolation of spatial data: some theory for kriging*. Springer, N.Y., 1999.
- [8] Douglas Nychka, Christopher Wikle, and J Andrew Royle. Multiresolution models for nonstationary spatial covariance functions. *Statistical Modelling*, 2(4):315–331, 2002.
- [9] Carling C Hay, Eric Morrow, Robert E Kopp, and Jerry X Mitrovica. Probabilistic reanalysis of twentieth-century sea-level rise. *Nature*, 2015.
- [10] S. Amari. *Differential geometry in statistical inference*, volume 10. Inst of Mathematical Statistic, 1987.
- [11] Geir-Arne Fuglstad, Daniel Simpson, Finn Lindgren, and Håvard Rue. Non-stationary spatial modelling with applications to spatial prediction of precipitation. *arXiv preprint arXiv:1306.0408*, 2013.
- [12] M. Calvo and J. Oller. An explicit solution of information geodesic equations for the multivariate normal model. *Statistics and Decisions*, 9:119–138, 1991.
- [13] C. Lenglet, M. Rousson, R. Deriche, and O. Faugeras. Statistics on the manifold of multivariate normal distributions: Theory and application to diffusion tensor mri processing. *Journal of Mathematical Imaging and Vision*, 25(3):423–444, 2006.
- [14] M. Fréchet. Les éléments aléatoires de nature quelconque dans un espace distancié. 1948.
- [15] H. Karcher. Riemannian center of mass and mollifier smoothing. *Communications on pure and applied mathematics*, 30(5):509–541, 1977.
- [16] Vincent Arsigny, Pierre Fillard, Xavier Pennec, and Nicholas Ayache. Log-euclidean metrics for fast and simple calculus on diffusion tensors. *Magnetic resonance in medicine*, 56(2):411–421, 2006.
- [17] Bertil Matérn et al. Spatial variation. stochastic models and their application to some problems in forest surveys and other sampling investigations. *Meddelanden fran statens Skogsforskningsinstitut*, 49(5), 1960.
- [18] WR Peltier. Global glacial isostasy and the surface of the ice-age earth: the ice-5g (vm2) model and grace. *Annu. Rev. Earth Planet. Sci.*, 32:111–149, 2004.
- [19] Simon J Holgate, Andrew Matthews, Philip L Woodworth, Lesley J Rickards, Mark E Tamisiea, Elizabeth Bradshaw, Peter R Foden, Kathleen M Gordon, Svetlana Jevrejeva, and Jeff Pugh. New data systems and products at the permanent service for mean sea level. *Journal of Coastal Research*, 29(3):493–504, 2012.
- [20] Neil Lawrence, Matthias Seeger, and Ralf Herbrich. Fast sparse gaussian process methods: The informative vector machine. In *Proceedings of the 16th Annual Conference on Neural Information Processing Systems*, number EPFL-CONF-161319, pages 609–616, 2003.